SMASIS 2021-67596

EXPERIMENTAL STUDY OF NCM-SI BATTERIES WITH BI-DIRECTIONAL ACTUATION

Shuhua Shan*

Department of Mechanical Engineering The Pennsylvania State University University Park, Pennsylvania 16802 Email: sxs2472@psu.edu

Cody Gonzalez

Department of Mechanical Engineering The Pennsylvania State University University Park, Pennsylvania 16802 Email: cag46@psu.edu

Christopher Rahn

Department of Mechanical Engineering The Pennsylvania State University University Park, Pennsylvania 16802 Email: cdr10@psu.edu

Mary Frecker

Department of Mechanical Engineering The Pennsylvania State University University Park, Pennsylvania 16802 Email: mxf36@psu.edu

ABSTRACT

Silicon is regarded as one of the most promising anode materials for lithium-ion batteries. Its high theoretical capacity (4000 mAh/g) has the potential to meet the demands of highenergy density applications, such as electric air and ground vehicles. The volume expansion of Si during lithiation is over 300%, indicating its promise as a large strain electrochemical actuator. A Si-anode battery is multifunctional, storing electrical energy and actuating through volume change by lithium-ion insertion.

To utilize the property of large volume expansion, we design, fabricate, and test two types of Si anode cantilevers with bi-directional actuation: (a) bimorph actuator and (b) insulated double unimorph actuator. A transparent battery chamber is fabricated, provided with NCM cathodes, and filled with electrolyte. The relationship between state of charge and electrode deformation is measured using current integration and high-resolution photogrammetry, respectively. The electrochemical performance, including voltage versus capacity and Coulombic efficiency versus cycle number, is measured for

several charge/discharge cycles. Both configurations exhibit deflections in two directions and can store energy. In case (a), the largest deflection is roughly 35% of the cantilever length. Twisting and unexpected bending deflections are observed in this case, possibly due to back-side lithiation, non-uniform coating thickness, and uneven lithium distribution. In case (b), the single silicon active coating layer can deflect 12 passive layers.

1. INTRODUCTON

Silicon is a promising high-capacity anode material in lithium-ion batteries. Its theoretical capacity (4000mAh/g) [1] makes it suitable for high-energy applications when paired with common cathodes. The volume expansion during lithium intercalation in silicon particles is over 300%, indicating its promise as a large strain electrochemical actuator.[2] [3] Sibased electrochemical actuators could provide significant advantages over existing actuation approaches, such as piezoelectric materials and shape memory alloys. [4] The fully lithiated Si exhibits around 45% maximum actuation strain while actuating at much lower voltage (< 4.5V) [5], much higher than piezoelectric polymer (0.02%-0.1%) and shape memory alloy (0.7%-7%) under high driving voltages [6]. Even though the large volume change during lithiation and delithiation results in cracks that cause poor reversibility and declining capacity [7]

^{*}Address all correspondence to this author.

[8], researchers have found that below the critical particle size of 150 nm, particle cracking can almost be eliminated [9].

Fig. 1 shows the concept of a multifunctional battery that can store electrical energy and actuate through volume change by lithium-ion insertion. The anodes are clamped at one end and free to deflect at the other end. During charge, Li ions migrate from the cathode (not shown), through the electrolyte, and into the Si particles. The Si volume expansion caused by lithium-ion intercalation results in longitudinal elongation of the active material layer. With the Cu passive layer axial constraint, the Si anode deflects away from the charging cathode. During discharge, delithiation of the Si anode causes the contraction of the active material layer, reversing the bending movement.

Previous research with unimorph cantilevers shows bilayer electrodes, consisting of an electrode layer and a current collector, can generate remarkable curvature changes through stress at the interface between the active layer and the passive layer. Ma *et al.* [5] revealed that Si composite electrode could bend laterally approximately 40% of beam length deflection at 60% SOC. Li *et al.* [10] found that the bending curvature of graphite composite electrodes could be controlled by adjusting state of charge (SOC) and the thickness ratio between the electrode layer and Cu foil. Xie *et al.* [11] found that the bending deformation of a mesocarbon microbead (MCMB) composite electrode cantilever depended on the graphite intercalation compound stage behavior.

Unimorph cantilevers deflect in only one direction. In this paper, we propose a bimorph design with active material on both sides of the current collector to provide bi-directional actuation with twice the deflection amplitude. Two bi-directional actuators are studied: (a) bimorph actuator and (b) insulated double

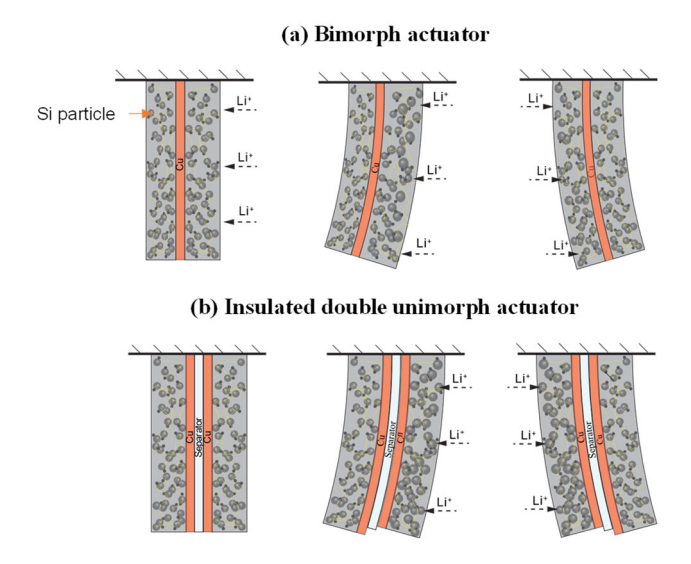


FIGURE 1: MULTIFUNCTIONAL NCM-SI BATTERY CONCEPT. (A) BIMORPH ACTUATOR; (B) INSULATED DOUBLE UNIMORPH ACTUATOR.

unimorph actuator. In case (a), differential lithiation of Si particles on both sides of the anode causes bi-directional actuation. For example, if the cathode is closer to the left side active materials, lithium ions preferentially insert in the left side of the anode due to the shorter path from the source [12], driving the electrode towards right. To avoid the backside lithiation [13] that can occur in case (a), bi-directional movement is realized by two unimorph actuators placed back-to-back with an insulating separator in between in case (b). A surrounding separator pouch mechanically connects the two unimorphs. When the right anode is lithiated, the expanded active material bends the passive layers towards left. The electrodes can reverse the deflection by discharge, and further shift to the right by charging the left anode.

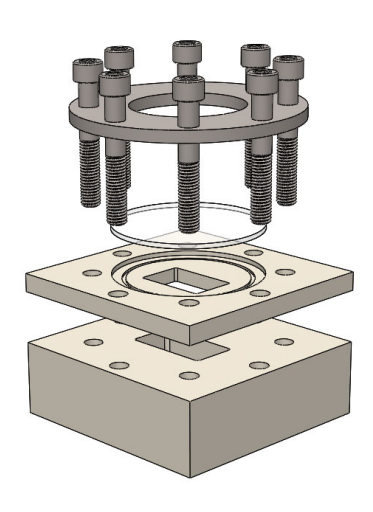


FIGURE 2: EXPLODED VIEW OF TRANSPARENT BATTERY

In this paper, we design, fabricate, and test these two types of Si anode cantilevers with bi-directional actuation and observe their deflection in a transparent battery. Measurements of voltage and displacement are collected via precision charging and discharging equipment and a macro-lens digital camera, respectively.

2. MULTIFUNCTIONAL BATTERY DESIGN AND FABRICATION

The transparent battery is presented in Fig. 2. The battery consists of eight stainless steel bolts with nuts, a polylactic acid (PLA) press ring, a borosilicate glass disk and two polypropylene (PP) pieces. The dimensions of the upper PP piece were 15.24cm×15.24cm×1.27cm. A circular step (Ø 10.16cm×0.32cm) and a concentric square through hole (50.00cm×31.75cm×35.00cm) were fabricated to accommodate a borosilicate glass disk and enable visualization of the battery deformation. The dimensions of the lower PP piece were

15.24cm×15.24cm×5.08cm. A chamber (6.00cm×3.18cm×3.50cm) was machined on the lower piece to house the battery. To prevent electrolyte leakage from the reaction chamber and the upper piece and from the upper piece and the borosilicate glass, two O-ring grooves (8.78cmOD×8.35cmID×0.13cm, 10.71cmOD×10.28cmID×0.13cm) were machined on both sides of the upper piece. Two FEP-encapsulated silicone O-rings (8.57cmOD × 8.26cmID × 0.16cm,

0.48cmOD×10.16cmID×0.16cm) were pressed into the grooves. The transparent battery was tightened and sealed by the eight bolts and nuts and the press ring.

The two types of multifunctional batteries were fabricated utilizing commercially available single-side-coated LiNiCoMnO₂ (5:2:3) cathodes (MTI). The NCM active material loading is 12.1 mg/cm². The Al foil thickness is 15 μ m, and the coating thickness is approximately 45 μ m.

Si single-side-coated anodes were prepared by mixing Si nanopowder (<100 μm , VWR), carbon black (MTI), and polyacrylic acid binder (Sigma-Aldrich) with a mass ratio of 6:2:2 to form a slurry. The solid content of the slurry was 25%. The slurry was cast on a 9 μm or 17 μm thick copper foil using a doctor blade. The electrodes were dried at 100 °C under vacuum. For Si double-side-coated anodes, the same process was repeated on the other side of the Cu foil. The average coating thickness of the double-side-coated anode in case (a) was 20 μm and 24 μm , respectively. The Cu foil thickness was 9 μm . The corresponding mass loadings were 0.973 mg/cm² and 1.327 mg/cm². The average coating thickness of the single-side-coated anode in case (b) was 19 μm , and the Cu thickness was 17 μm . The mass loading was 0.885 mg/cm².

In case (a), the NCM cathodes (2cm × 3cm) were inserted into separator pouches (Celgard 2325) and attached to two sides of the chamber with Loctite E-120HP Hysol epoxy adhesive to provide electrical insulation from the anodes. The double-sidecoated anode was cut into a 3cm × 5mm strip and placed between the two cathodes. In case (b), Si anodes and NCM cathodes were cut into two $3.5 \text{cm} \times 4 \text{mm}$ strips and two $3.5 \text{cm} \times 6 \text{mm}$ strips, respectively. Two Si anodes were placed with the active materials facing outward. Two cathodes were placed with the NCM coating layers facing the Si active materials to provide shortest paths for lithium-ion migration. Each electrode was insulated by a separator layer (4cm × 8mm) to avoid direct contact during deformation. All the separator layers were heat sealed together at the tips, and a green strapping tape was placed at the tip location as a tip marker. The 13-layer configuration is shown in Fig. 3 (right side).

In both cases, each anode and cathode was connected to Cu wires with polytetrafluoroethylene (PTFE) insulation and Al wires with polyvinyl chloride (PVC) insulation, respectively. The conductivity between wires and electrodes were achieved by mechanical tightening of chemical-resistant screws with nuts. A 3D-printed PP clamp was fabricated to fix the deformed electrodes into position. It was attached to the top of the test chamber by epoxy. After installing all the electrodes into the chamber, the wire hole was sealed with epoxy.

After assembly, the transparent battery was dried at 60 °C under vacuum for 12 hours. The transparent battery was then transferred into an Argon filled glovebox (< 0.1 PPM O_2 and < 0.1 PPM H_2O) for electrolyte injection. The electrolyte was 1M LiPF₆ in EC/DEC (v/v 1:1, Sigma-Aldrich). The electrolyte was injected through a port in the lower PP piece. After filling, the port was sealed with a chemical-resistant tapered plug.

3. EXPERIMENTAL SETUP

The experimental setup is shown in Fig. 3. The cycling tests were carried out on a Landt A2000 battery test system at room temperature. The tip displacement was captured every 3 minutes by a macro-lens digital camera. In both configurations, gravity loading was minimized by orienting the electrodes vertically.

In case (a), two cathodes and the anode were connected to the tester together to charge both sides of the anode. Galvanostatic cycling was carried out at approximately C/22 rate. The cell was fully charged and discharged for 3 cycles. To further investigate lithium-ion distribution, only one cathode and the anode were cycled in the following cycles.

In case (b), only one Si anode and the closest NCM cathode were connected to the tester. Galvanostatic cycling was performed at approximately C/39. For the left side, the Si anode was charged at constant current (CC) 0.1mA for 14 hours, followed by a constant discharge 0.1mA to cutoff voltage (2V)

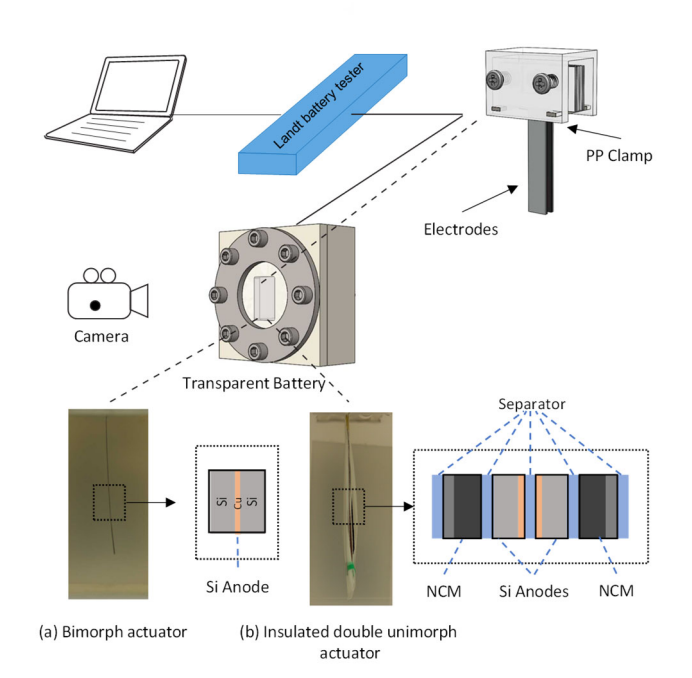


FIGURE 3: EXPERIMENTAL SETUP.

in the 1st cycle. In the 2nd cycle, only a CC charge was performed until the voltage reached 4V, and then discharged. In the following cycles, after a CC charge, a constant voltage charge (CV) was applied at 4V until the charging current decreased to 0.01 mA. For the right side, a galvanostatic charge at 0.1 mA was carried out for 22 hours and followed by a full discharge. In the following cycles, a CC/CV charge was applied to 4V with a cutoff current 0.01mA. The full charge capacity of Si anodes (2.69 mAh/mg) was measured by using CR2016 coin cells with lithium foil as the counter electrode. The maximum state of charge (SOC) of the two anodes in the 1st cycle were approximately 36% SOC and 43% SOC.

4. RESULTS AND DISCUSSION

4.1 Bimorph actuator

Galvanostatic cycling was carried out at 0.25 mA to 100% SOC for the first cycle. The anode was placed approximately in the middle of the two cathodes. The tip position of the uncharged anode was set to be the initial position. The voltage profile and

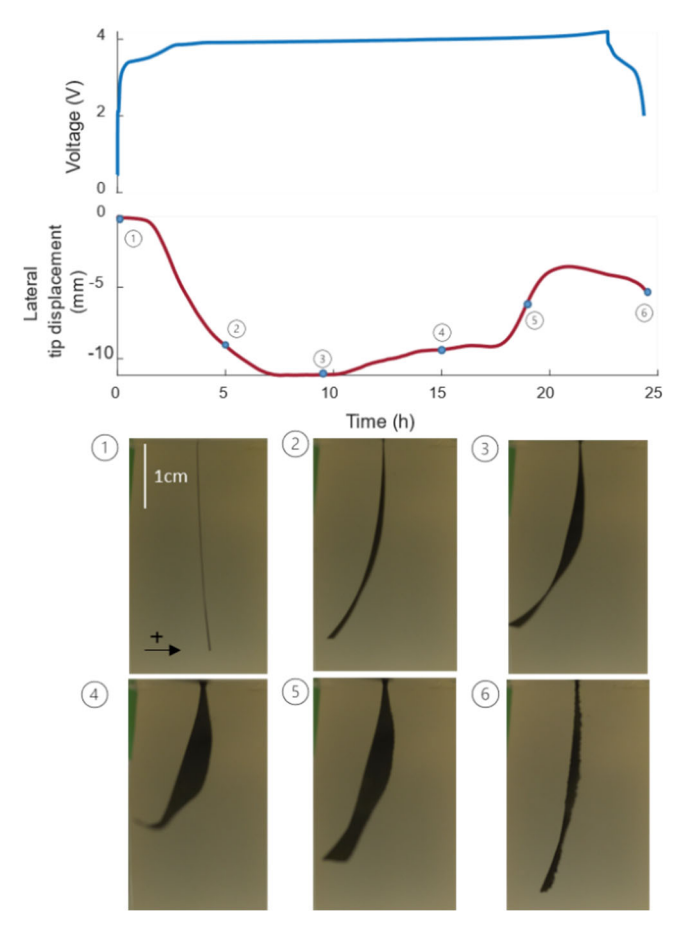


FIGURE 4: VOLTAGE PROFILE, LATERAL TIP DISPLACEMENT AND DEFLECTION PHOTOS IN THE FIRST CYCLE OF THE BIMORPH ACTUATOR.

the corresponding lateral tip deflection curve in the 1st cycle are shown in Fig 4, with some deflection photos presented. The initial curvature of the unloaded Si anode (photo 1) was due to binder swelling in the electrolyte and different thickness of the two coating layers. [5] In the range of 0% SOC to 18.2% SOC (photo 2), the Si anode deformed towards to the left. The anode started to twist while moving further to the left until approximately 36.3% SOC (photo 3). The tip eventually touched the left side of the chamber. Instead of lateral deflection, it started to move upward from 36.3% SOC to roughly 50.0% SOC. Meanwhile, the twist became more pronounced than that in the lower SOC as shown in the photo 4. From 50.0% SOC to 84.1% SOC, the tip changed its moving direction to the right (photo 5). The tip started to move to the left until 100% SOC charge. The tip further deflected to the left until discharge (photo 6). The maximum lateral tip displacement was roughly 35% of the cantilever length.

The first leftward deflection at low SOC can be explained by the thickness difference of coating layers that results in unequal mechanical properties of the two sides. The left coating layer has smaller stiffness than the right one due to smaller coating thickness. When both sides are lithiated and experiencing volume expansion under the same charge condition, the anode tends to move towards the side with less stiffness. Twist was observed after 18.2% SOC. This is possibly related to uneven lithiation and unequal coating thickness across the anode width. The non-uniform coating thickness along the width possibly accelerates the twist due to uneven lithiation. After the tip reached to its left limit, the tip exhibited rightward deflection and less twist, which might be caused by active material delamination and lithium-ion redistribution within the Si anode. [14] The unsmooth surface observed on the right side of the bimorph actuator in photo 6 shows that part of the active material separated from the Cu current collector during cycling, while the left side did not exhibit obvious delamination. Meanwhile, the Li ion redistribution in the active material might help to even the ununiform load along the anode width. Li ions migrate from locations of high concentration to those of low

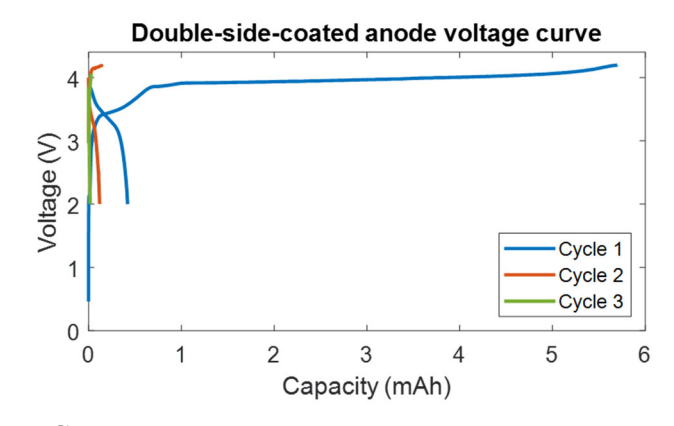


FIGURE 5: ELECTROCHEMICAL PERFORMANCE OF THE BIMORPH ACTUATOR.

concentrations in the anodes and alleviate the induced twist by uneven lithiation.

The electrochemical performance of the first three cycles is presented in Fig. 5. The fast decay of capacity after the 1st cycle is due to active material delamination.

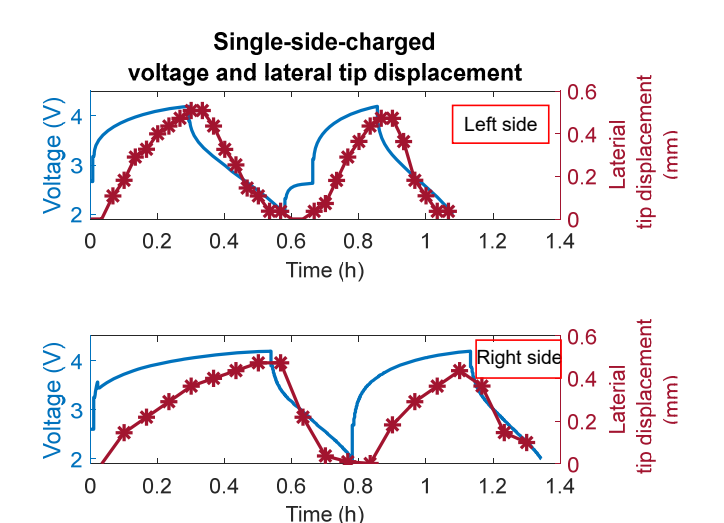


FIGURE 6: LATERAL TIP DISPLACEMENT UNDER SINGLE-SIDE-CHARGED CONDITION

To investigate lithium distribution within the two coating layers, galvanostatic cycling tests at 0.1 mA were performed on the left-side electrode pair and the right-side electrode pair. In the tests, the distances between the two coating layers with the Li ion source were not the same. Li ions tend to insert into the closest active material as it provides a straight path with much faster and more efficient Li ion transport. Thus, the tip is expected to move towards different directions when Li ions come from different locations. Fig. 6 shows the voltage profiles and corresponding tip lateral displacements. The transparent battery was charged to 4V and fully discharge for 2 cycles. Unexpectedly, the tip deflection was only one-directional when the corresponding side of the anode was closer to the Li ion source. The maximum tip displacement was approximately 0.5mm rightward in both cases, indicating that when the Li ion source is closer to the right-side active material, the left-side Si particles far away from the Li ion source are also lithiated, reducing the anode deflection. Some Li ions detour around the facing active material and insert into the back-side Si particles as shown in Fig. 7. It also helps to explain why the tip further moved to the left even though the left-side Si was closer to the cathode in the 1st cycling test as shown in Fig. 4. The right-side Si far away from the Li ion source is also lithiated, causing the continued leftward deflection. Our finding is consistent with back-side lithiation phenomenon reported in batteries with the graphite anodes. [13]

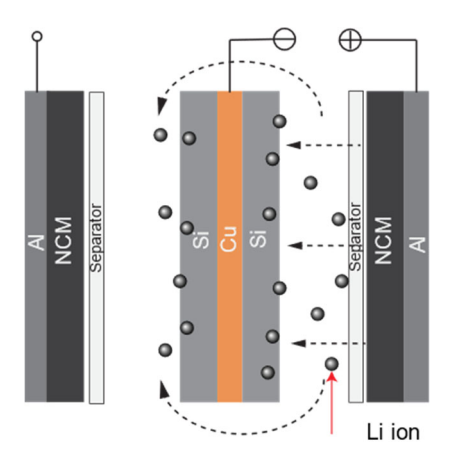


FIGURE 7: BACK-SIDE LITHIATION PHENOMENON

4.2 Insulated double unimorph actuator

The first 3 cycles electrochemical performance of both sides of the insulated double unimorph actuator are presented in Fig.8. The charge and discharge curves in (a) (b) show that the transparent battery can store and release energy during cycling. As shown in (c-e), the charge capacities in the 1st cycle of both anodes were 1.3559 mAh (36% SOC) and 1.6009 mAh (43% SOC), and the discharge capacities were 0.4880 mAh and 0.4826 mAh, respectively. The corresponding Coulombic efficiencies were 35.99% and 30.15%. After the 1st cycle, the Coulombic efficiencies of the two sides went up and stabilized at approximately 70% and 50%. The low Coulombic efficiency in the 1st cycle can be explained by solid electrolyte interphase (SEI) formation. SEI is a passivation layer on the anode surface that formed from electrolyte decomposition in the first few cycles. SEI formation and growth consumes lithium ions and electrolyte materials irreversibly, making low Coulombic efficiency in the first few cycles. [15] After the 2nd cycle, both cases showed a decreased efficiency and then stabilized. This is due to the active material delamination that was observed in the experiment. [16] Part of the active material detached from the Cu current collector during lithiation. In coin cells and pouch cells, pressure is applied to preserve electrode integrity. Since the anodes in the transparent box are free-standing with no applied pressure, the Si particles can separate from the Cu current collector due to volume expansion and contraction in cycling. The electrode fracture and active material delamination cause the irreversible loss of lithium ions in anodes, generating low discharge capacity. The stabilized Coulombic efficiency is possibly due to the completion of SEI formation.

The transparent battery's bi-directional tip deflections are shown in Fig. 9. The initial position of the tip in each test was set to be zero. It shows that the 19µm Si coating layer deflected 12 passive layers with approximately 273µm total thickness in two directions. The transparent battery deflected away from the initial position during lithiation and moved back during

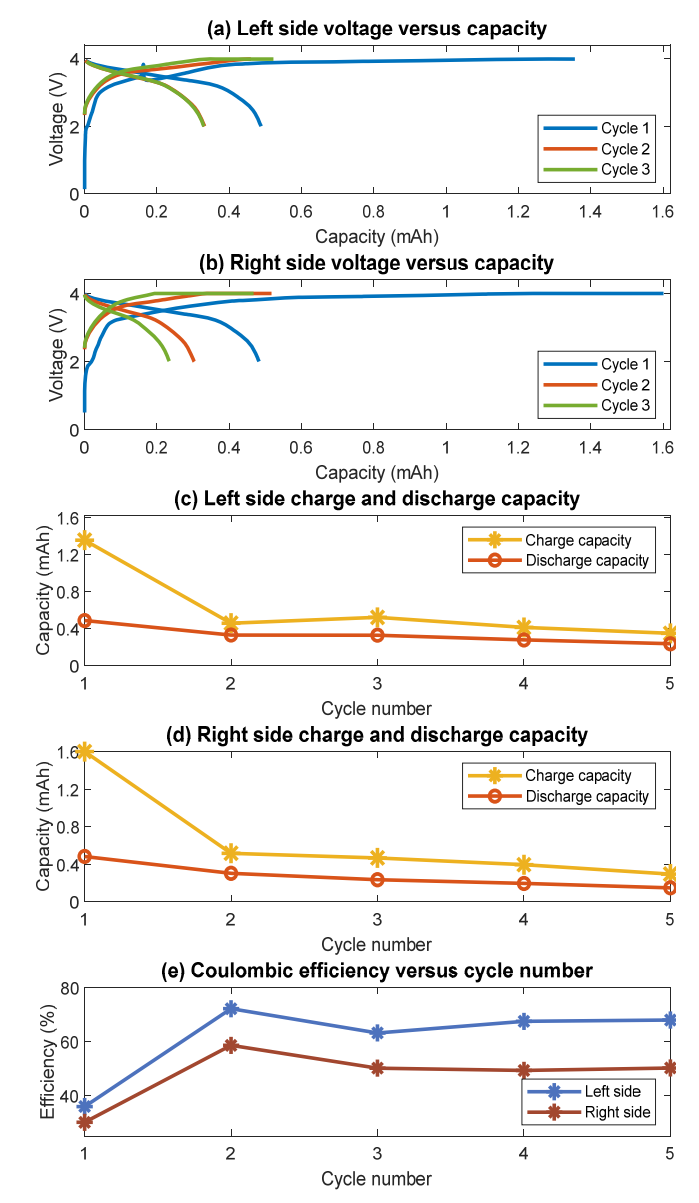


FIGURE 8: ELECTROCHEMICAL PERFORMANCE OF THE INSULATED DOUBLE UNIMORPH ACTUATOR.

delithiation. For the left side, the maximum tip displacement was approximately 1.142 mm. For the right side, the maximum tip displacement was roughly 0.592mm. The difference between two sides' tip displacements is possibly due to the misalignment of electrodes and ununiform gaps between electrode layers. The electrode tip did not always return to its initial position. This might come from two effects. First, the Cu current collector may experience plastic deformation during volume expansion of Si particles. Second, the SEI layer formed on the anode surface and residual Li ions trapped in Si particles may change the mechanical properties of the anodes, making it unable to deform back to its initial position.[17]

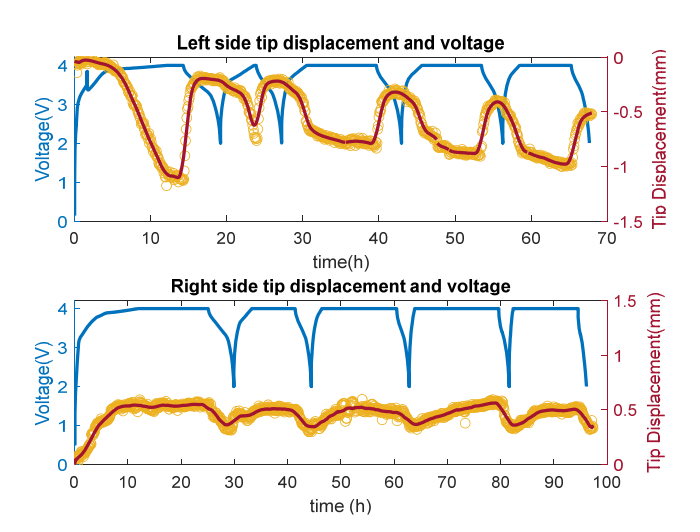


FIGURE 9: LATERAL TIP DISPLACEMENT OF THE INSULATED DOUBLE UNIMORPH ACTUATOR.

5. Conclusions

This paper presented two types of Si anode configurations that stored energy and achieved bi-directional actuation through volume expansion and contraction associated with Li ion intercalation. The bimorph actuator stored 5.697 mAh (charge)/0.421 mAh (dishcharge) with tip deflection of approximately 35% of the beam length. For the insulated double unimorph actuator, the two Si anodes in the transparent battery stored 1.3559 mAh (charge)/0.4880 mAh (discharge) capacity and 1.6009 mAh (charge)/0.4826 mAh (discharge) capacity, respectively. The single Si active coating layer deflected 12 passive layers with maximum tip deflection of 1.142 mm at 36% SOC. This study demonstrates multifunctionality of the NCM-Si battery and the promise of the Si anode as a bi-directional electrochemical actuator.

In the bimorph configuration, actuation was difficult to control due to back-side lithiation. In the insulated double unimorph configuration, the two Si anodes deflected with respect to their own neutral axis, and the tip movement was difficult to capture because of the limited deflection with 12 passive layers. Future work may focus on combining two Si anodes with a symmetric configuration separated by a non-conductive, chemically compatible adhesive layer that is compliant enough to visualize large beam deflection.

ACKNOWLEDGEMENT

The authors gratefully acknowledge the support of the National Science Foundation under Grant No. 1662055.

REFERENCES

- [1] Ozanam, F., and Rosso, M., 2016, "Silicon as Anode Material for Li-Ion Batteries," Mater. Sci. Eng. B Solid-State Mater. Adv. Technol., 213, pp. 2–11.
- [2] Lang, J., Ding, B., Zhu, T., Su, H., Luo, H., Qi, L., Liu, K., Wang, K., Hussain, N., Zhao, C., Li, X., Gao, H., and Wu, H., 2016, "Cycling of a Lithium-Ion Battery with a Silicon Anode Drives Large Mechanical Actuation," Adv. Mater., 28(46), pp. 10236–10243.
- [3] Gonzalez, C., Ma, J., Frecker, M., and Rahn, C., 2020, "Analytical Modeling and Simulation of a Multifunctional Segmented Lithium Ion Battery Unimorph Actuator," Smart Mater. Struct.
- [4] Chin, T. E., Rhyner, U., Koyama, Y., Hall, S. R., and Chiang, Y.-M., 2006, "Lithium Rechargeable Batteries as Electromechanical Actuators," Electrochem. Solid-State Lett., 9(3), p. A134.
- [5] Ma, J., Gonzalez, C., Huang, Q., Farese, J., Rahn, C., Frecker, M., and Wang, D., 2020, "Multifunctional Li(Ni0.5Co0.2Mn0.3) O2-Si Batteries with Self-Actuation and Self-Sensing," J. Intell. Mater. Syst. Struct., 31(6), pp. 860–868.
- [6] Huber, J. E., Fleck, N. A., and Ashby, M. F., 1997, "The Selection of Mechanical Actuators Based on Performance Indices," Proc. R. Soc. A Math. Phys. Eng. Sci., 453(1965), pp. 2185–2205.
- [7] Kalnaus, S., Rhodes, K., and Daniel, C., 2011, "A Study of Lithium Ion Intercalation Induced Fracture of Silicon Particles Used as Anode Material in Li-Ion Battery," J. Power Sources, **196**(19), pp. 8116–8124.
- [8] Chae, S., Ko, M., Kim, K., Ahn, K., and Cho, J., 2017, "Confronting Issues of the Practical Implementation of Si Anode in High-Energy Lithium-Ion Batteries," Joule, 1(1), pp. 47–60.
- [9] Liu, X. H., Zhong, L., Huang, S., Mao, S. X., Zhu, T., and Huang, J. Y., 2012, "Size-Dependent Fracture of Silicon," ACS Nano, 6(2), pp. 1522–1531.
- [10] Li, D., and Wang, Y., 2020, "Communication— Controllable Deformation of Composite Graphite Electrodes during Electrochemical Process," J. Electrochem. Soc., 167(14), p. 140511.
- [11] Xie, H., Song, H., Kang, Y., and Wang, J., 2018, "In Situ Experimental Measurement of the Mechanical Properties of Carbon-Based Electrodes during the Electrochemical Process," J. Electrochem. Soc., 165(10), p. A2069.
- [12] Lee, Y., Son, B., Choi, J., Kim, J. H., Ryou, M. H., and Lee, Y. M., 2015, "Effect of Back-Side-Coated Electrodes on Electrochemical Performances of Lithium-Ion Batteries," J. Power Sources, 275, pp. 712–719.
- [13] Lee, Y., Son, B., Choi, J., Kim, J. H., Ryou, M. H., and Lee, Y. M., 2015, "Effect of Back-Side-Coated Electrodes on Electrochemical Performances of

- Lithium-Ion Batteries," J. Power Sources, **275**, pp. 712–719.
- [14] Basak, S., Migunov, V., Tavabi, A. H., George, C., Lee, Q., Rosi, P., Arszelewska, V., Ganapathy, S., Vijay, A., Ooms, F., Schierholz, R., Tempel, H., Kungl, H., Mayer, J., Dunin-Borkowski, R. E., Eichel, R. A., Wagemaker, M., and Kelder, E. M., 2020, "Operando Transmission Electron Microscopy Study of All-Solid-State Battery Interface: Redistribution of Lithium among Interconnected Particles," ACS Appl. Energy Mater., 3(6), pp. 5101–5106.
- [15] Nadimpalli, S. P. V, Sethuraman, V. A., Dalavi, S., Lucht, B., Chon, M. J., Shenoy, V. B., and Guduru, P. R., 2012, "Quantifying Capacity Loss Due to Solid-Electrolyte-Interphase Layer Formation on Silicon Negative Electrodes in Lithium-Ion Batteries," J. Power Sources.
- [16] Tariq, F., Yufit, V., Eastwood, D. S., Merla, Y., Biton, M., Wu, B., Chen, Z., Freedman, K., Offer, G., Peled, E., Lee, P. D., Golodnitsky, D., and Brandon, N., 2014, "In-Operando X-Ray Tomography Study of Lithiation Induced Delamination of Si Based Anodes for Lithium-Ion Batteries," ECS Electrochem. Lett., 3(7).
- [17] Xie, H., Qiu, W., Song, H., and Tian, J., 2016, "In Situ Measurement of the Deformation and Elastic Modulus Evolution in Si Composite Electrodes during Electrochemical Lithiation and Delithiation," J. Electrochem. Soc., 163(13), p. A2685.